CrystEngComm

Accepted Manuscript

ROYAL SOCIETY OF CHEMISTRY

www.rsc.org/crystengcomm

Cite this: DOI: 10.1039/c0xx00000x

www.rsc.org/ crystengcomm

ARTICLE TYPE

The thermodynamics characteristics of organic crystals growth by physical vapor transport: towards high-quality and color-tunable crystal preparation

Huan Wang,*[a] Yang Zhao,[a] Zengqi Xie,[b] Huaiyuan Wang,*[a] Baohui Wang[a] and Yuguang Ma[bc]

Received (in XXX, XXX) Xth XXXXXXXXX 20XX, Accepted Xth XXXXXXXXX 20XX
DOI: 10.1039/b000000x

In this work, several organic crystals of anthracene (Ac), tetracene (Tc), pentacene (Pc) and 2,5-diphenyl-1,4- distyrylbenzene with two trans double bonds (DPDSB) have been prepared by the physical vapor transport (PVT) method. The structural characteristics of these crystals are investigated by atomic force microscopy (AFM) and X-ray diffraction (XRD). In the PVT method, the growth temperature decides the kinetic energy of molecules and the disturbance of crystal lattices caused by intermolecular interactions during the crystal formation process. The crystal grown from the lower temperature has the smaller monolayer thickness and the narrower full width at half maximum (FWHM) calculated from diffraction peak degrees given by XRD data, which indicates the molecules are arranged more orderedly, compared with the crystal grown from the higher temperature. Based on the crystal growth thermodynamics characteristics in vapor, Tc doped Ac crystals with partial energy transfer (sky-blue emission) and nearly complete energy transfer (green emission) have been prepared corresponding to the low temperature and high temperature growth conditions, respectively. The photoluminescence efficiencies of Tc doped Ac crystals with sky-blue emission and green emission are ~40% and ~74%, the energy transfer efficiencies are 63.8% and 98.9%, respectively. Our results are relevant to the understanding of organic crystal growth thermodynamics behaviors and guide us the design and preparation of color-tunable emission and high-luminescence efficiency organic crystals that are expected to be of interest for organic light emitting transistors, diodes and lasers.

Introduction

Organic single crystals constructed by π-conjugated molecules have attracted great attention in the field of organic optoelectronic materials.[1-4] The academic motivation for organic single crystal research is their definite structures, which provides a model to investigate the basic interactions between the molecules (supramolecular interaction), and the relationship between molecular stacking modes and optoelectronic performance (luminescence and carrier mobility).[5,6] In the meanwhile, the superiorities of organic crystals such as high thermal stability, high ordered structure and high carrier mobility make them attractive candidates for optoelectronic devices such as optically pumped lasers,[7,8] field-effect transistors,[9-11] electroluminescence,[12] and photovoltaic cell.[13] The excellent quality of organic crystal is important to the performance of optoelectronic devices based on the crystals. Commonly, physical vapor transport (PVT) is an effective approach to grow the large-size, smooth-surface organic crystals which are more suitable to be used in the device fabrication. It has been verified that the crystals grown from PVT possess nice laser properties, such as the larger gain, the smaller loss and the lower threshold of amplified spontaneous emission (ASE), which is attributed to the more regular shapes and smoother surfaces of these crystals which are more beneficial for self-waveguided emission and propagation.[14,15] Most of reported organic crystals used to field-effect transistors with high carrier mobilities were prepared by PVT, such as rubrene single crystal hole mobility was as high as 20 cm^2/Vs and the perylene derivative (PDIF-CN_2) single crystal electron mobility could be up to 6 cm^2/Vs.[16,17] Recently, high-luminescence doped organic crystals prepared by PVT have received significant attentions.[18-20] The structural comparability of host and guest molecules is important for large-size doped crystal growth as well as structural-order retention. And the definite molecular stacking orientation in the doped crystal provides a model to investigate the relationship of spatial orientation and energy transfer properties.[21] Doped organic crystals with structural-order retention as the combination of high luminescence and high mobility have been used to light emitting transistors,[22] which are expected to be towards electrically pumped organic lasers. Therefore, PVT is an important method to grow high quality organic single crystals or doped crystals, but the characteristics of crystal formation[23-25] and growth temperature effects[26,27] which benefit for the development of crystal engineering[28] are reported rarely.

In this work, several organic crystals of Ac, Tc, Pc and

DPDSB are prepared by PVT method, and the temperature effects on the crystal growth behaviors are discussed. It is found that the crystal grown from the lower temperature has the smaller monolayer thickness and the narrower FWHM by the AFM and XRD analyses, which indicates the crystal quality is higher. According to the crystal growth thermodynamics characteristics, the Tc doping quantities in the Tc doped Ac crystals (abbreviated as Ac⊂Tc crystals) could be modulated by controlling the growth zone temperature. Based on the steady-state and time-resolved fluorescence measurements, Ac⊂Tc crystal grown from the high temperature presents the green emission with nearly complete energy transfer because the disturbance of crystal lattice caused by the binding energy release of intermolecular interactions is more intense and Tc molecules with higher kinetic energy are more easily embedded into the Ac crystal under the high temperature condition. Correspondingly, Ac⊂Tc crystal grown from the low temperature presents the sky-blue emission with partial energy transfer due to the less Tc doping quantities. The preliminary result verifies that the temperature condition could control the doping content of guest molecules which benefit to realize the color-tunable emission and high-luminescence efficiency in the doped organic crystal.

Experimental section

UV-vis absorption and fluorescence spectra were recorded on UV-3100 and RF-5301PC spectrophotometer respectively. Crystalline state photoluminescent (PL) efficiencies were measured in an integrating sphere.[29] Atomic force microscopy (AFM) images were recorded under ambient conditions using a Digital Instrument Multimode Nanoscope IIIa operating in the tapping mode. Si cantilever tips (TESP) with the resonance frequency of approximately 300 kHz and the spring constant of about 40 N/m were used. The wide-angle X-ray diffraction was detected with a Rigaku X-ray diffractometer (D/Max-rA, using Cu-Kα radiation of wavelength 1.542 Å), and in the test the slice crystal was flatted parallel to the single-crystal Si substrate.

Time-resolved fluorescence measurements were performed by the time-correlated single photon counting (TCSPC) system under right-angle sample geometry. A 379 nm picosecond diode laser (Edinburgh Instruments EPL375, repetition rate 20MHz) were used to excite the sample. The emission was detected by a photomultiplier tube (Hamamatsu H5783p) and a TCSPC board (Becker&Hickel SPC-130). The instrument response function (IRF) is about 220 ps. All the measurements were carried out at room temperature (22°C).

Anthracene, tetracene and pentacene, purchased from J&K ACROS (98%), were purified by sublimation few times before use. DPDSB was synthesized and purified as referred in our previous work.[30]

Results and discussions

1. Preparation of the crystals

The crystal growth apparatus was reported in our previous work as shown in Figure 1.[25] The sublimation temperatures of Ac, Tc, Pc and DPDSB were 170 ºC, 200 ºC, 300 ºC and 220 ºC in the source zone, respectively. And their molecular structures are shown in Chart 1. The sublimated molecules transport with carrier gas (Ar, 99.999%), and then the crystals grow in the growth zone. After two or three days of stable growth, the large-size slice crystals formed hanging inside of the growth tube. A series of crystals could be obtained from the high to the low temperature gradient with the increasing dimensions in the growth zone. Some of these crystals are chosen to their structural analyses.

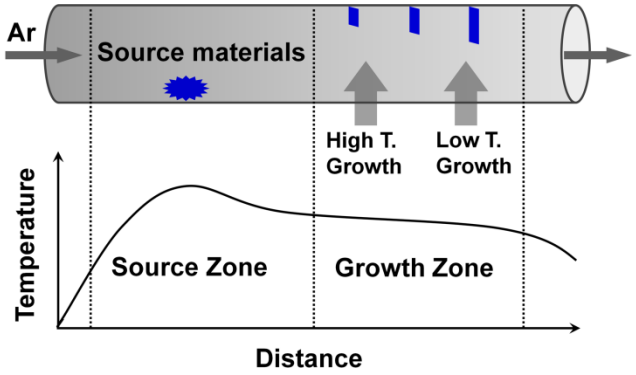

Fig. 1 Schematics of the apparatus for the growth of organic crystals by physical vapor transport method. The temperature in the apparatus is controlled as shown in the bottom.

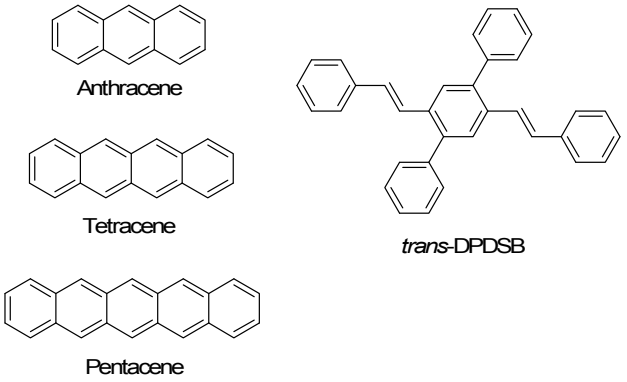

Chart 1 Molecular structures of anthracene, tetracene, pentacene and *trans*-DPDSB.

2. Morphology and structure of the crystals

The crystals of Ac, Tc, Pc and DPDSB all have the slice-like shapes, smooth surfaces and larger sizes of several millimeters. Figure 2 shows their optical photographs. Tapping-mode AFM has been used to observe the flat areas of crystal surfaces with scanning range 5×5 μm^2. From the AFM height images in Figure 3, step-like morphologies have been found. From their cross-section analyses, the average heights of steps observed on the crystal surfaces of Ac, Tc, Pc and DPDSB are about 1.06, 1.39, 1.64 and 1.32 nm, respectively.

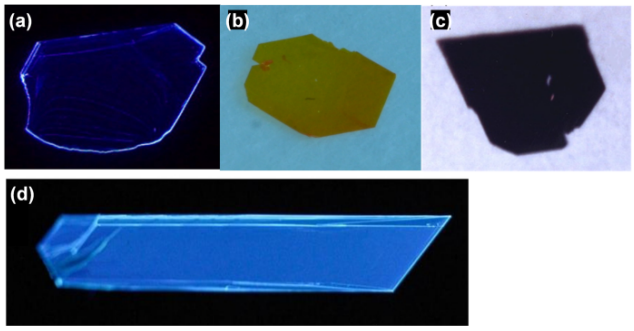

Fig. 2 Optical photographs of the anthracene crystal (a), tetracene crystal (b), pentacene crystal (c) and DPDSB crystal (d); and (a), (d) under the ultraviolet lamp.

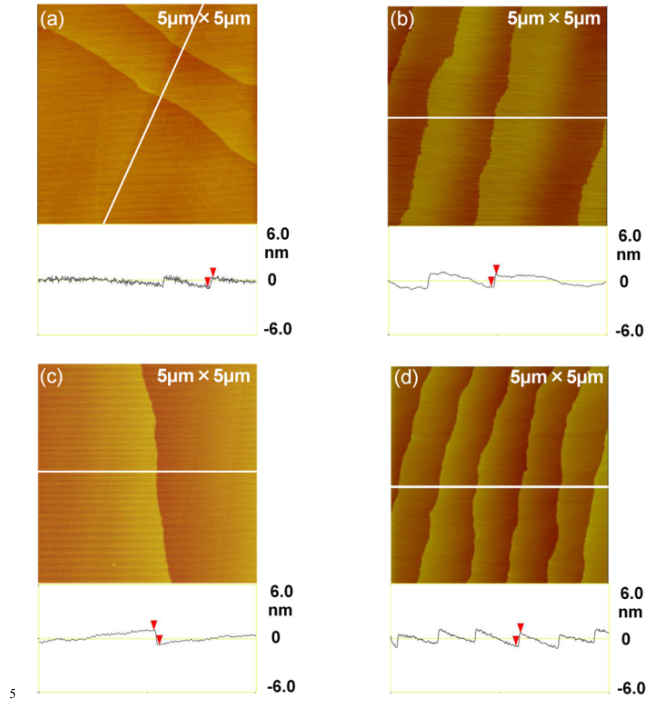

Fig. 3 The crystal surface AFM height images of anthracene (a), tetracene (b), pentacene (c) and DPDSB (d); and their cross-section analyses shown in the bottom of images.

Figure 4 shows the comparisons of XRD patterns of the Ac crystals (a), Tc crystals (b), Pc crystals (c) and DPDSB crystals (d) grown from the low temperature and the high temperature, respectively. In the experiment, the crystal was parallel to the single-crystal Si substrate, so that equidistant diffraction peaks from the layer-by-layer structures vary with angle. According to the Bragg equation, the monolayer thicknesses of Ac, Tc, Pc and DPDSB crystals grown from the low temperature (the high temperature) are calculated to be 9.06 (9.25), 12.14 (12.18), 14.16 (14.35) and 11.31 (11.57) Å, respectively, which correspond to the one-step height of these crystals in the AFM image. In the case of DPDSB crystal, the unit cell parameters obtained from the Cambridge Structural Database (CSD) are a = 6.67 Å, b = 8.03 Å, c = 11.71 Å, α = 80.01 º, β = 83.27 º, γ = 83.93 º. Comparing with the XRD results (Fig. 4d), we notice that the primary diffraction spacing is approximately identical to the unit cell parameter c (11.71 Å). This indicates that the layer-by-layer growth in the crystal is along the c axis, of the DPDSB molecules. The results of AFM morphologies and XRD patterns suggest that all the crystals have a layer-by-layer structure and each layer corresponds to a molecular monolayer. The crystal growth temperature conditions, first diffraction peak degrees, calculated monolayer thicknesses and first diffraction peak FWHMs are summarized in Table 1.

Diffraction peak FWHMs data could be denoted as $\Delta(2\theta)$, which reflect the crystalline ordering. The crystals grown from the low temperature have the smaller monolayer thickness and the narrower FWHM, which indicate the molecules are arranged more orderedly. In other words, the quality of the crystal grown from the low temperature is higher than that grown from the high temperature. The molecular arrangement ordering could be described by the Scherrer equation,

$$\tau = \frac{K\lambda}{\beta \cos\theta} \quad (1)$$

τ is the mean size of the ordered (crystalline) domains, which can reflect the molecular stacking ordering. K is a dimensionless shape factor, with a typical value of about 0.9. λ is the X-ray wavelength; β is the FWHM and θ is the Bragg angle. It can be seen that the diffraction peak FWHM is smaller and the diffraction degree is larger, and the crystal quality is higher. The growth temperature will influence the disturbance of crystal lattices caused by the binding energy release of intermolecular interactions during the crystal formation process. So when the temperature is higher, the disturbance of crystal lattices will be more intense and the molecular arrangement ordering will be declining.

Using the temperature effects on the crystal growth behaviors in the PVT method, the Tc molecules are successfully doped in the Ac crystals with different doping quantities by controlling the growth zone temperature. In the growth zone with the high temperature, the disturbance of crystal lattice is more intense and Tc molecules with higher kinetic energy are more easily embedded into the Ac crystal than that in the growth zone with the low temperature. So the quantities of Tc molecules are more in the Ac⊂Tc crystal grown from the high temperature (Figure 5c). According to the crystal growth thermodynamics characteristics, the doped organic crystals prepared by PVT can realize color-tunable emissions using the energy transfer. The green emission Ac⊂Tc crystal has been grown from the temperature of about 100 ºC. Figure 5a shows the XRD patterns of the green emission Ac⊂Tc crystal, compared with that of the pure Ac crystal. The molecular monolayer thickness of Ac⊂Tc crystal is calculated to be 9.20 Å, which is close to the value of pure Ac crystal grown from the high temperature of 100 ºC (9.25 Å). It is indicated that the higher growth temperature intensifies the disturbance of crystal lattice and gives the guest Tc molecules higher kinetic energy to incorporate into the host Ac crystal lattice. Figure 5b shows the AFM height image of Ac⊂Tc crystal surface, and its step average height from the cross-section analysis is nearly similar to the step height of pure Ac crystal (1.06 nm) which also corresponds to a molecular monolayer. The results of XRD patterns and AFM morphology suggest that the structural ordering of the host Ac crystal has been retained after doping a certain quantity of tetracene molecules into it, which

could ensure the high carrier mobility in the doped crystals.

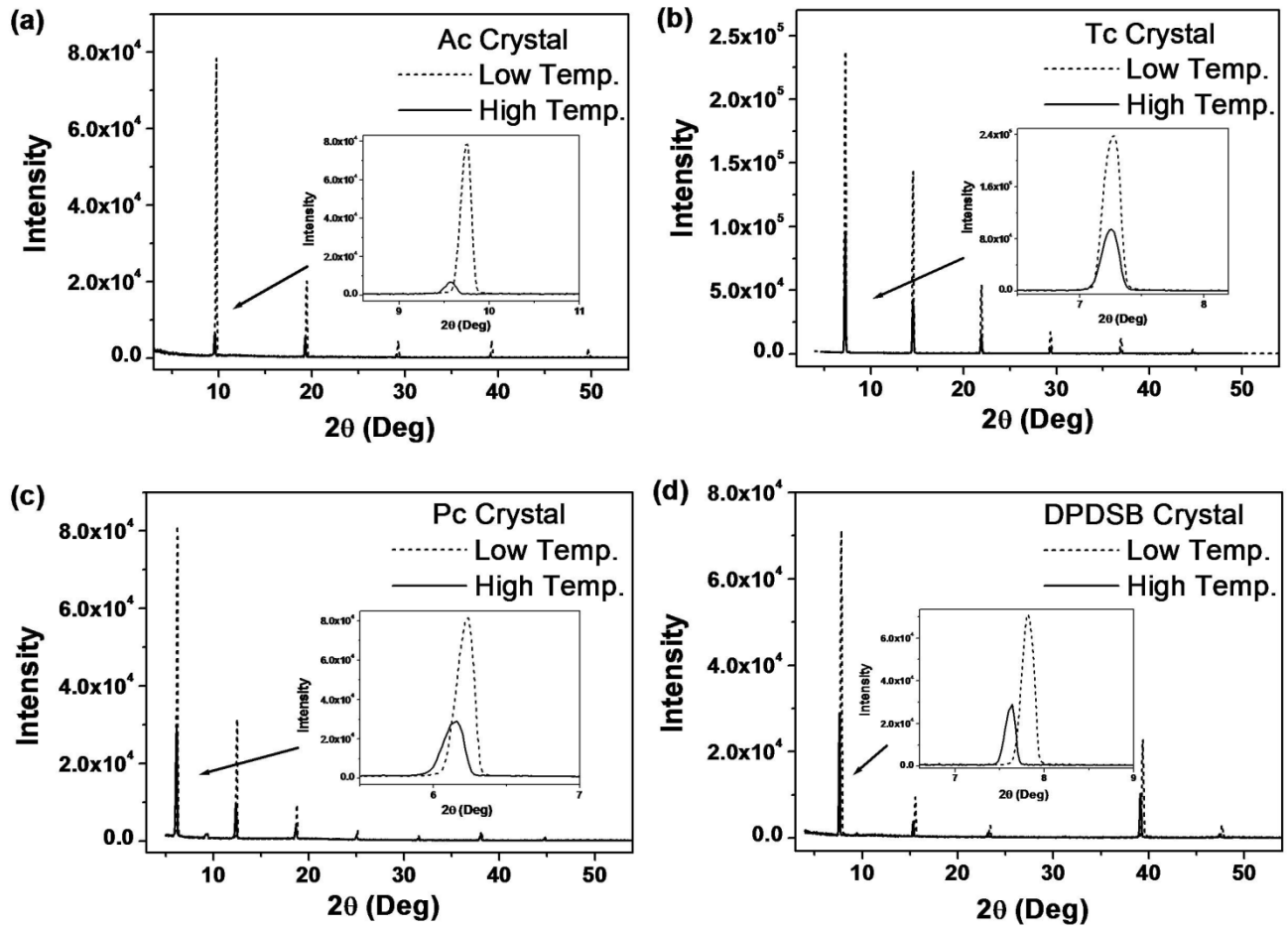

Fig. 4 Comparisons of XRD patterns of the anthracene crystals (a), tetracene crystals (b), pentacene crystals (c) and DPDSB crystals (d) grown from the low temperature and the high temperature, respectively. Insert figures are the first diffraction peaks.

Table 1 Summary of growth zone temperatures, first diffraction peak degrees, molecular monolayer thicknesses and first diffraction peak FWHMs of several crystals.

Crystal	Growth zone temperature T (ºC)	Diffraction degree 2θ (º)	Molecular monolayer thickness d (Å)[a]	FWHM β (º)
Ac	Low Temp. (70)	9.76	9.06	0.135
	High Temp. (100)	9.56	9.25	0.140
Tc	Low Temp. (140)	7.28	12.14	0.158
	High Temp. (170)	7.26	12.18	0.162
Pc	Low Temp. (250)	6.24	14.16	0.142
	High Temp. (280)	6.16	14.35	0.170
DPDSB	Low Temp. (170)	7.82	11.31	0.150
	High Temp. (200)	7.64	11.57	0.154

[a] The calculated molecular monolayer thickness corresponded well with the step height observed by AFM, but generally ~0.2 nm smaller than AFM results, due to systematic error of the instrument in the process of scanning AFM images.

3. Steady-state fluorescence

The sublimation temperatures for Tc and Ac are about 200 and 170 °C in the source zone, respectively. The green emission Ac⊂Tc crystal and sky-blue emission Ac⊂Tc crystal could be obtained at the temperatures of about 100 and 70 ºC in the growth zone, respectively. Figure 6a shows the emission spectra of Ac⊂Tc crystals prepared in the low temperature (70 ºC) and the high temperature (100 ºC), respectively, which include the host Ac emission bands peaking at 423, 442 and 470 nm, and the guest Tc emission bands peaking at 494, 529 and 570 nm. The photoluminescence (PL) spectrum of green emission Ac⊂Tc crystal shows that the emission mainly comes from Tc molecules verifying the nearly complete energy transfer. And the sky-blue emission Ac⊂Tc crystal shows the partial energy transfer with the host Ac emission residual. Figure 6b shows the emission spectrum of pure Ac crystal, and both the absorption and emission spectrum of Tc in chloroform ($CHCl_3$). It can be seen that there is a big overlap between the PL spectrum of Ac crystal and the absorption spectrum of Tc, which ensures the efficient

energy transfer from the host Ac to the guest Tc. The absorption spectrum of Tc displays a well-resolved vibrational energy band in the range of 400−500 nm which indicates the characteristic of a rigid, planar, one-dimensional π-system. The PL spectrum of Tc in dilute solution presents three emission bands peaking around 481, 511, and 548 nm, respectively, which are mirror-plane symmetrical with the absorption spectra and are assigned as the transition from the first excited-state S1 to the ground-state S0 with varied vibrational levels as 0-0, 0-1 and 0-2 transition, respectively. The emission peaks of Tc in the Ac⊂Tc crystal have about 20 nm red shifts relative to that of Tc in solution, such as the 0-1 transition emissions of Tc in the Ac⊂Tc crystal and in the solution are 529 and 511 nm, respectively. That may be caused by the conjugated effect of Tc with the surrounding Ac molecules.

As we know, the herringbone arrangement of Tc molecules in the solid state can quench the luminescence sharply, so the luminescent efficiency of Tc in the aggregated state is no more than 1%.[31] But doping Tc into the Ac crystal could effectively avoid the intermolecular aggregates. The crystalline-state PL efficiencies of Ac⊂Tc crystals measured in an integrating sphere are as high as 40% for the sky-blue emission and 74% for the green emission, respectively. With the variations of temperature gradient in the growth zone, a series of different color emission Ac⊂Tc crystals can be obtained with the different Tc doping quantities by the PVT method. It is based on the crystal growth thermodynamics characteristics that the temperature decides the disturbance of host-crystals lattice inducing the guest molecules embedment.

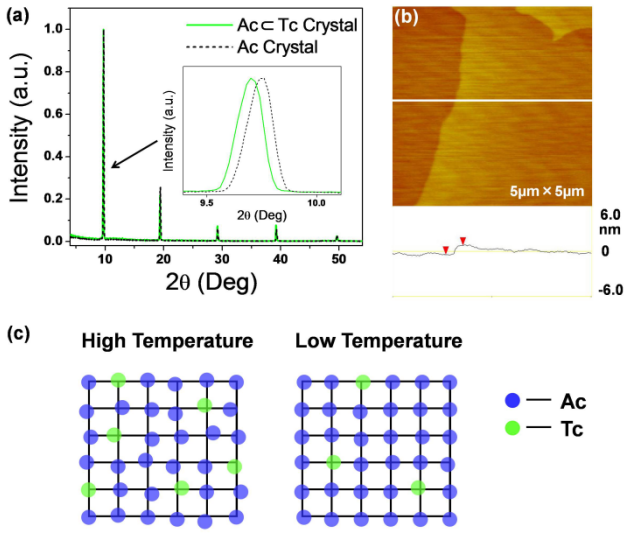

Fig. 5 (a) XRD patterns of the Ac⊂Tc crystal and Ac crystal, and insert figure is the first diffraction peaks. (b) The AFM height image of Ac⊂Tc crystal surface, and the cross-section analysis shown in the bottom of image. (c) Schematics of the disturbance of crystal lattices when Tc molecules are doped into the Ac crystal at the high temperature and the low temperature, respectively.

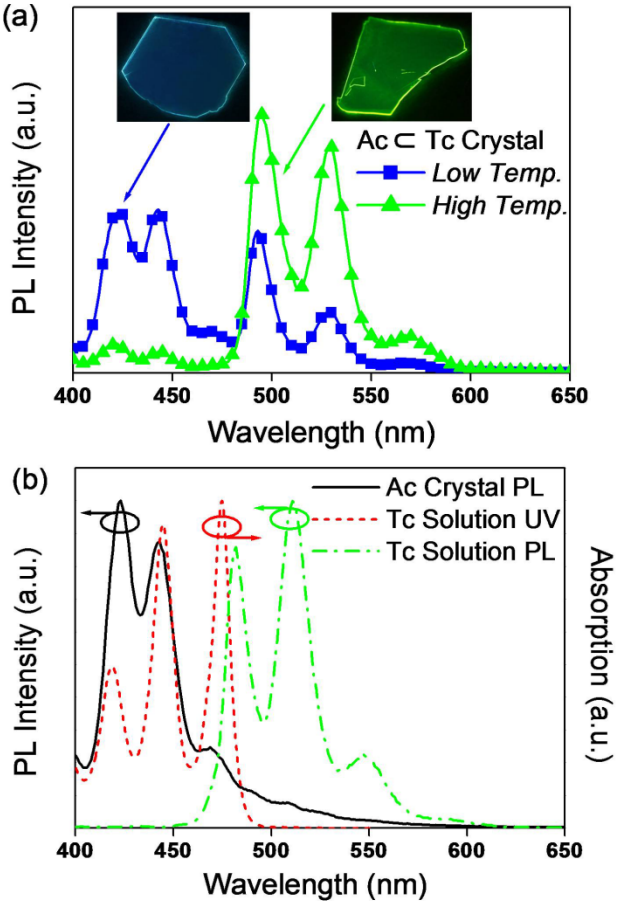

Fig. 6 (a) The emission spectra of Ac⊂Tc crystals prepared in the low temperature (70 ºC) and the high temperature (100 ºC), respectively. Inserts are the optical photographs of Ac⊂Tc crystals corresponding to the emission spectra. (b) The emission spectrum of Ac crystal, and the emission and absorption spectrum of Tc solution (chloroform as the solvent).

4. Time-resolved fluorescence

The time-resolved fluorescence is an effective method to explore the energy transfer in the doped system. Figure 7a shows the PL decay curves of the pure Ac crystal, Ac⊂Tc crystals grown from the low temperature (sky-blue emission) and the high temperature (green emission) respectively, monitored at 423 nm that is one of the emission peaks of the Ac crystal. The decay time of the pure Ac crystal is about 10.30 ns, while it is decreased to 3.71 ns of the sky-blue emission Ac⊂Tc crystal and 0.11 ns of the green emission Ac⊂Tc crystal with an increase of Tc doping quantities. The decreased decay time in the doping crystals clearly verifies the energy transfer process as discussed in the above section. The rate of energy transfer from a donor to an acceptor k_{ET} is given by

$$k_{ET} = \frac{1}{\tau_D}\left(\frac{R_0}{R}\right)^6 \quad (2)$$

where τ_D is the decay time of the donor in the absence of acceptor, R_0 is the Förster distance, and R is the donor-to-acceptor distance. The transfer rate k_{ET} can be calculated from the decay times measured in the absence (τ_D) and presence (τ_{DA}) of acceptor: $k_{ET} = 1/\tau_{DA} - 1/\tau_D$. For the sky-blue emission Ac⊂Tc crystal and

the green emission Ac⊂Tc crystal, the k_{ET} is equal to 1.72×10^{8} s^{-1} and 8.99×10^{9} s^{-1}, respectively. And the efficiency of energy transfer Φ_{ET} is given by

$$\Phi_{ET} = \frac{k_{ET}}{k_{ET} + \frac{1}{\tau_D}} \quad (3)$$

Thus, the Φ_{ET} is 63.8% for the sky-blue emission Ac⊂Tc crystal and 98.9% for the green emission Ac⊂Tc crystal, respectively. The decay time of the acceptor Tc in Ac matrix is remarkably prolonged from 14.15 to 18.79 ns with an increase of Tc doping quantities monitored at the emission wavelength of 529 nm (Figure 7b). This indicates Tc molecules are embedded in Ac crystal with approximately uniform dispersion. A summary of transient PL decay times for Ac crystal, Ac⊂Tc crystals grown from the low temperature (sky-blue emission) and the high temperature (green emission) respectively is given in Table 2.

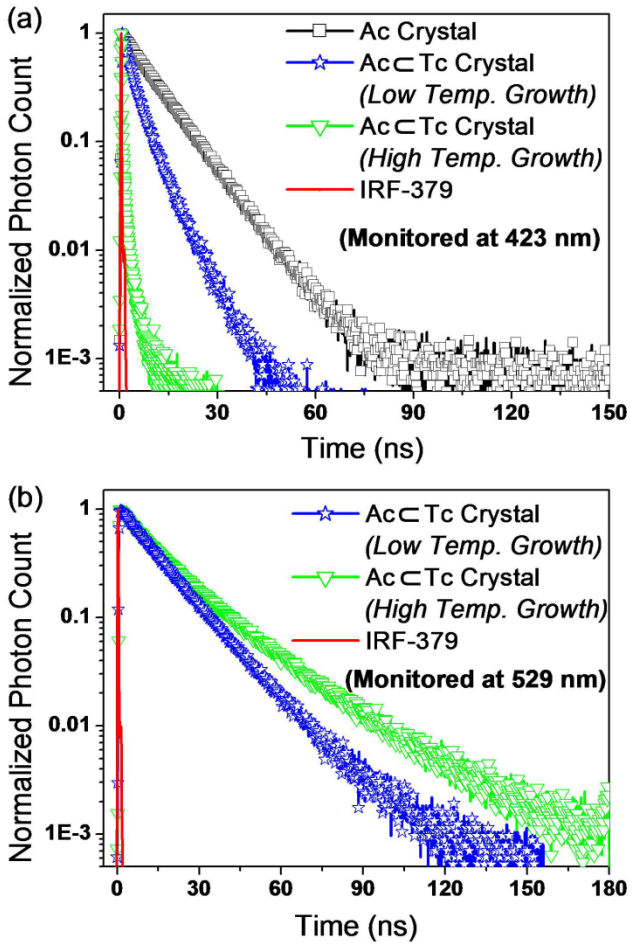

Fig. 7 Time-resolved fluorescences of Ac crystal, Ac⊂Tc crystals grown from the low temperature and the high temperature respectively at different emission wavelengths. (a) λ_{em} = 423 nm; (b) λ_{em} = 529 nm.

Table 2 Decay data of Ac crystal, Ac⊂Tc crystals grown from the low temperature (sky-blue emission) and the high temperature (green emission) respectively.

Crystal (emission color)[a]	Decay time τ (ns)	Percentage (%)	Mean lifetime τ (ns)	Emission wavelength λ_{em} (nm)
Ac	10.30	100	10.30	423 nm
Ac⊂Tc (sky-blue)	6.19	40.64	3.71	
	2.02	59.36		
Ac⊂Tc (green)	0.083	97.34	0.11	
	0.91	2.53		
	6.21	0.13		
Ac⊂Tc (sky-blue)	13.12	90.06	14.15	529nm
	23.48	9.94		
Ac⊂Tc (green)	2.76	9.56	18.79	
	12.90	58.48		
	26.93	31.97		

[a] Mol ratios of Tc to Ac in Ac⊂Tc crystals are estimated by the chromatograph. For the sky-blue emission Ac⊂Tc crystal, n_{Tc}: n_{Ac} = 1: 41; for the green emission Ac⊂Tc crystal, n_{Tc}: n_{Ac} = 1: 12.

Conclusions

Several organic crystals have been prepared by the PVT method under the low temperature and the high temperature growth conditions, respectively. Their structural characteristics investigated by XRD have been compared and it is found that the crystal grown from the low temperature has the smaller monolayer thickness and the narrower FWHM, which indicate the molecules are arranged more orderedly and the crystal quality is higher, compared with the crystal grown from the high temperature. Using the temperature effects on the crystal growth behaviors, the Tc molecules are successfully doped in the Ac crystals with color-tunable emissions by controlling the growth zone temperature. Ac⊂Tc crystals realize the high luminescence using the energy transfer verified by steady-state and time-resolved fluorescences. Our experimental results are relevant to the understanding of organic crystal growth thermodynamics behaviors and guide us the design and preparation of color-tunable emission and high-luminescence efficiency organic crystals that are expected to be of interest for organic light emitting transistors, diodes and lasers.

Acknowledgements

We are grateful for financial support from the National Science Foundation of China (51175066, 91233113), National Basic Research Program of China (973 Program) (2013CB834705), National Young Top Talents Plan of China (2013), New Century Excellent Talents in University (NCET-12-0704), Guangdong Natural Science Foundation (grant number S2012030006232), Introduced Innovative R&D Team of Guangdong (201101C0105067115) and PCSIRT.

Notes and references

[a] *College of Chemistry and Chemical Engineering, Northeast Petroleum University, Daqing, 163318, P. R. China. Fax: (+86)459-6504154; Tel: (+86)459-6504154; E-mail: wanghuan83214@gmail.com, wanghyjiji@163.com*

[b] *State Key Laboratory of Luminescent Materials and Devices, Institute of Polymer Optoelectronic Materials and Devices, South China University of Technology, Guangzhou 510640, P. R. China.*

[c] State Key Laboratory of Supramolecular Structure and Materials, Jilin University, Changchun 130012, P. R. China.

1 M. Pope, H. P. Kallmann and P. Mangnante, *J. Chem. Phys.,* 1963, **38**, 2042.
2 O. S. Avanesjan, V. A. Benderskii, V. K. Brikenstein, V. L. Broude, L. I. Korshunov, A. G. Lavrushko and I. I. Tartakovskii, *Mol. Cryst. Liq. Cryst.,* 1974, **29**, 165.
3 D. Fichou, S. Delysee and J. M. Nunzi, *Adv. Mater.,* 1997, **9**, 1178.
4 V. Y. Butko, X. Chi and A. P. Ramirez, *Solid State Commun,* 2003, **128**, 431.
5 C. Reese and Z. N. Bao, *J. Mater. Chem.,* 2006, **16**, 329.
6 Z. Q. Xie, B. Yang, F. Li, G. Cheng, L. L. Liu, G. D. Yang, H. Xu, L. Ye, M. Hanif, S. Y. Liu, D. G. Ma and Y. G. Ma, *J. Am. Chem. Soc.,* 2005, **127**, 14152.
7 H. Yanagi, T. Ohara and T. Morikawa, *Adv. Mater.,* 2001, **13**, 1452.
8 M. Ichikawa, R. Hibino, M. Inoue, T. Haritani, S. Hotta, T. Koyama and Y. Taniguchi, *Adv. Mater.,* 2003, **15**, 213.
9 V. C. Sundar, J. Zaumseil, V. Podzorov, E. Menard, R. L. Willett, T. Someya, M. E. Gershenson and J. A. Rogers, *Science,* 2004, **303**, 1644.
10 A. L. Briseno, S. C. B. Mannsfeld, M. M. Ling, S. Liu, R. J. Tseng, C. Reese, M. E. Roberts, Y. Yang, F. Wudl and Z. N. Bao, *Nature,* 2006, **444**, 913.
11 S. C. B. Mannsfeld, B. C-K. Tee, R. Stoltenberg, C. V. H-H. Chen, S. Barman, B. V. O. Muir, A. N. Sokolov, C. Reese and Z. N. Bao, *Nat. Mater.,* 2010, **9**, 859.
12 Y. Hisao, M. Takayuki and S. Hotta, *Appl. Phys. Lett.,* 2002, **81**, 1512.
13 R. J. Tseng, R. Chan, V. C. Tung and Y. Yang, *Adv. Mater.,* 2008, **20**, 435.
14 W. J. Xie, F. Li, H. Wang, Z. Q. Xie, F. Z. Shen, Y. G. Ma and J. C. Shen, *APPLIED OPTICS*, 2007, **46**, 4431.
15 H. Wang, F. Li, I. Ravia, B. R. Gao, Y. P. Li, V. Medvedev, H. B. Sun, N. Tessler and Y. G. Ma, *Adv. Funct. Mater.,* 2011, **21**, 3770.
16 V. Podzorov, E. Menard, A. Borissov, V. Kiryukhin, J. A. Rogers, M. E. Gershenson, *Phys. Rev. Lett.,* 2004, **93**, 086602.
17 A. S. Molinari, H. Alves, Z. H. Chen, A. Facchetti and A. F. Morpurgo, *J. Am. Chem. Soc.,* 2009, **131**, 2462.
18 Y. S. Zhao, H. B. Fu, F. Q. Hu, A. D. Peng, W. S. Yang and J. N. Yao, *Adv. Mater.,* 2008, **20**, 79.
19 H. Wang, F. Li, B. R. Gao, Z. Q. Xie, S. J. Liu, C. L. Wang, D. H. Hu, F. Z. Shen, Y. X. Xu, H. Shang, Q. D. Chen, Y. G. Ma and H. B. Sun, *Cryst. Growth Des.,* 2009, **9**, 4945.
20 H. H. Fang, S. Y. Lu, L. Wang, R. Ding, H. Y. Wang, J. Feng, Q. D. Chen and H. B. Sun, *Org. Electron.,* 2013, **14**, 389.
21 H. Wang, B. L. Yue, Z. Q. Xie, B. R. Gao, Y. X. Xu, L. L. Liu, H. B. Sun and Y. G. Ma, *Phys. Chem. Chem. Phys.,* 2013, **15**, 3527.
22 H. Nakanotani, M. Saito, H. Nakamura and C. Adachi, *Adv. Funct. Mater.,* 2010, **20**, 1610.
23 S. Jo, H. Yoshikawa, A. Fujii and M. Takenaga, *Appl. Surf. Sci.,* 2006, **252**, 3514.
24 X. H. Zeng, Y. Qiu, J. Qiao, G. F. Dong and L. D. Wang, *Appl. Surf. Sci.* 2007, **253**, 3581.
25 H. Wang, Z. Q. Xie, B. Yang, F. Z. Shen, Y. P. Li and Y. G. Ma, *CrystEngComm,* 2008, **10**, 1252.
26 R. A. Laudise, C. Kloc, P. G. Simpkins and T. Siegrist, *J. Cryst. Growth,* 1998, **187**, 449.
27 Z. Q. Xie, Y. T. Wang, Y. G. Ma and J. C. Shen, *Synth. Met.,* 2003, **137**, 983.
28 R. J. Davey, K. Allen, N. Blagden, W. I. Cross, H. F. Lieberman, M. J. Quayle, S. Righini, L. Seton and G. J. T. Tiddy, *CrystEngComm,* 2002, **4**, 257.
29 Y. Kawamura, H. Sasabe and C. Adachi, *Jpn. J. Appl. Phys. Part 1,* 2004, **43**, 7729.
30 Z. Q. Xie, B. Yang, L. L. Liu, M. Li, D. Lin, G. Cheng, S. Y. Liu and Y. G. Ma, *J. Phys. Org. Chem.,* 2005, **18**, 962.
31 A. Tersigni, J. Shi, D. T. Jiang and X. R. Qin, *Phys. Rev. B*, 2006, **74**, 205326.

The table of contents entry

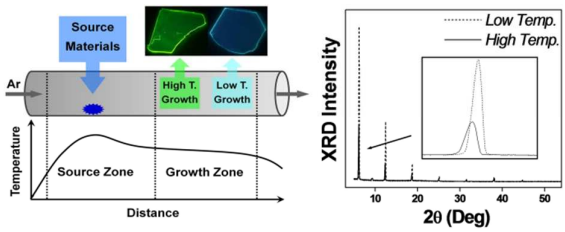

Organic crystal grown from the lower temperature has the tighter molecular stacking, the sharper diffraction peak and the higher quality.